Journal of
Nanoscience and Nanotechnology
Vol. 10, 355–359, 2010

Application of Hierarchical MFI Zeolite for the Catalytic Pyrolysis of Japanese Larch

Kyu-Hong Park[1], Hyun Ju Park[1], Jeongnam Kim[2], Ryong Ryoo[2], Jong-Ki Jeon[3], Junhong Park[4], and Young-Kwon Park[1,*]

[1] *Faculty of Environmental Engineering, University of Seoul, Seoul 130-743, Korea*
[2] *Center for Functional Nanomaterials and Department of Chemistry, KAIST, Daejeon 305-701, Korea*
[3] *Department of Chemical Engineering, Kongju National University, Gongju 341-701, Korea*
[4] *School of Mechanical Engineering, Hanyang University, Seoul 133-791, Korea*

The catalytic pyrolysis of Japanese larch was carried out over a hierarchical MFI zeolite (Meso MFI C16). The zeolite was synthesized using an amphiphilic organosilane as a mesopore-directing agent, and its catalytic activity was compared with that of the conventional HZSM-5 and the mesoporous material from HZSM-5 (MMZ_{ZSM-5}). The effect of the hierarchical MFI zeolite on the product distribution and chemical composition of the bio-oil was also examined. The hierarchical MFI zeolite exhibited the highest activity in deoxygenation and aromatization during the catalytic pyrolysis of Japanese larch. In particular, it showed high selectivity for valuable aromatics, such as benzene, toluene, and xylenes (BTX), even though it decreased the organic fraction of bio-oil. Its higher mesoporosity resulted, however, in an increase in the coke amount and in undesirable products, such as polycyclic aromatic hydrocarbons (PAHs).

Keywords: Hierarchical MFI Zeolite, Bio-Oil, Catalytic Pyrolysis, BTX Aromatics.

1. INTRODUCTION

The importance of alternative energy development has increased rapidly due to high international crude oil prices. Bio-oil has been recognized as a representative renewable energy source and chemical feedstock.

In the past few decades, several studies have examined the upgrading of bio-oil over solid acid catalysts, such as pure and modified zeolites.[1–8] According to these studies, HZSM-5 is the most effective catalyst for cracking or reforming bio-oil. However, HZSM-5 with micropores in the 5.1×5.6 Å size range is limited by its low mass transfer rate, particularly in the case of large molecules.

Since 1990, Kuroda et al. first reported the preparation of meosporous silica with uniform pore size distribution from the layered polysilicate kanemite (FSM-16), a variety of mesoporous materials (the M41S family, including MCM-41, MCM-48 and MCM-50, and HMS-, MSU-1, SBA-15, and MCF type materials) were synthesized. These mesoporous materials with regular geometries have recently gained much attention due to their great potential, in practical applications such catalyst, adsorption, separation, sensing, medical usage, ecology, and nanotechnology.[9] MCM-41 based materials have been examined as pyrolysis catalysts in biomass-derived vapors.[10, 11] Recently, the highly hydrothermal stable mesoporous aluminosilicates, MMZ and MSU-S materials, were applied to the catalytic pyrolysis of biomass.[12–14] However, the acidity of these mesoporous materials is still lower than that of microporous aluminosilicate zeolites, which may be a shortcoming in the upgrading of bio-oil. The more recently developed hierarchical MFI zeolites[15] have a high acidity and mesopores, and are expected to show the good activity in the catalytic pyrolysis of biomass.

This study attempted the catalytic pyrolysis of Japanese larch, which is well known as a representative wood species in Korea, over a hierarchical MFI zeolite. Its catalytic activity in terms of the effect on the product distribution and composition was also compared with that of an MMZ material and of conventional HZSM-5.

2. EXPERIMENTAL DETAILS

2.1. Catalyst Preparation

A hierarchical MFI zeolite with a Si/Al molar ratio of 20 was synthesized using the procedure described elsewhere.[15, 16] An amphiphilic organosilane, i.e., [(3-trimethoxysilyl)propyl] hexadecyldimethylammonium chloride(TPHAC), was used as a mesopore-directing

*Author to whom correspondence should be addressed.

 1533-4880/2010/10/355/005 doi:10.1166/jnn.2010.1537

agent. Hereinafter, the hierarchical MFI zeolite is referred to as "Meso MFI C16." For comparison, a mesoporous material from a zeolite (MMZ_{ZSM-5}) with a similar Si/Al molar ratio was prepared using the procedure reported elsewhere.[13, 14] A commercially available zeolite, HZSM-5 (Zeolyst International Company), and cetyltrimethylammonium bromide (CTAB) were used as the framework source and the template, respectively. All the catalysts thus obtained were calcined, ion exchanged with a 1.0 M ammonium nitrate solution at 80 °C repeatedly (4 times) to convert them into NH_4^+ form, and finally calcined again at 550 °C to convert them into H^+ form.

2.2. Characterization of Catalysts

The catalysts synthesized in this study were characterized as follows: N_2 adsorption/desorption isotherms were obtained at −196 °C with a Micromeritics ASAP 2000 with the Brunauer-Emmett-Teller (BET) surface area calculated from the linear portion of the BET plot. The micropore volume and the external surface area were evaluated using the *t*-plot method, and the pore size distribution was determined using the Brunauer-Joyner-Halenda (BJH) model. The acidity was investigated using the NH_3-temperature-programmed desorption (TPD) method with a TPD/TPR 2900 analyzer (Micromeritics Instrument Co.). Prior to the measurements, the samples were first treated in a He stream at 500 °C and cooled to 100 °C, after which NH_3 adsorption was carried out at this temperature. After the samples were purged in the He stream for 2 h to completely remove the physically adsorbed NH_3, the catalysts were heated to 700 °C at a heating rate of 10 °C/min. The desorbed NH_3 was detected using a thermal conductivity detector (TCD). Inductively coupled plasma analysis was used to determine the Si:Al molar ratio. After the upgrading, the coke amount deposited on the catalysts was determined with thermogravimetric analysis (TGA) using a thermogravimetric analyzer (TGA, [TGA 2050, TA Instruments]), in the presence of air, at a heating rate of 5 °C/min.

2.3. Reaction Procedure

Japanese larch was used in the catalytic upgrading of the wood-derived pyrolytic vapors. The sawdust used in these experiments was screened using standard sieves with sizes ranging from 0.425 to 1.0 mm, and dried in an oven (J-NDS1, JISICO) at 110 °C for 24 h to minimize water in the oil product. After the drying, the water contents in all the wood sawdust had less than 1 wt%.

The pyrolysis of the Japanese larch sawdust and the subsequent catalytic pyrolysis of the pyrolytic vapors were carried out in fixed bed reactor systems. Figure 1 shows a schematic diagram of the pyrolysis and catalytic pyrolysis

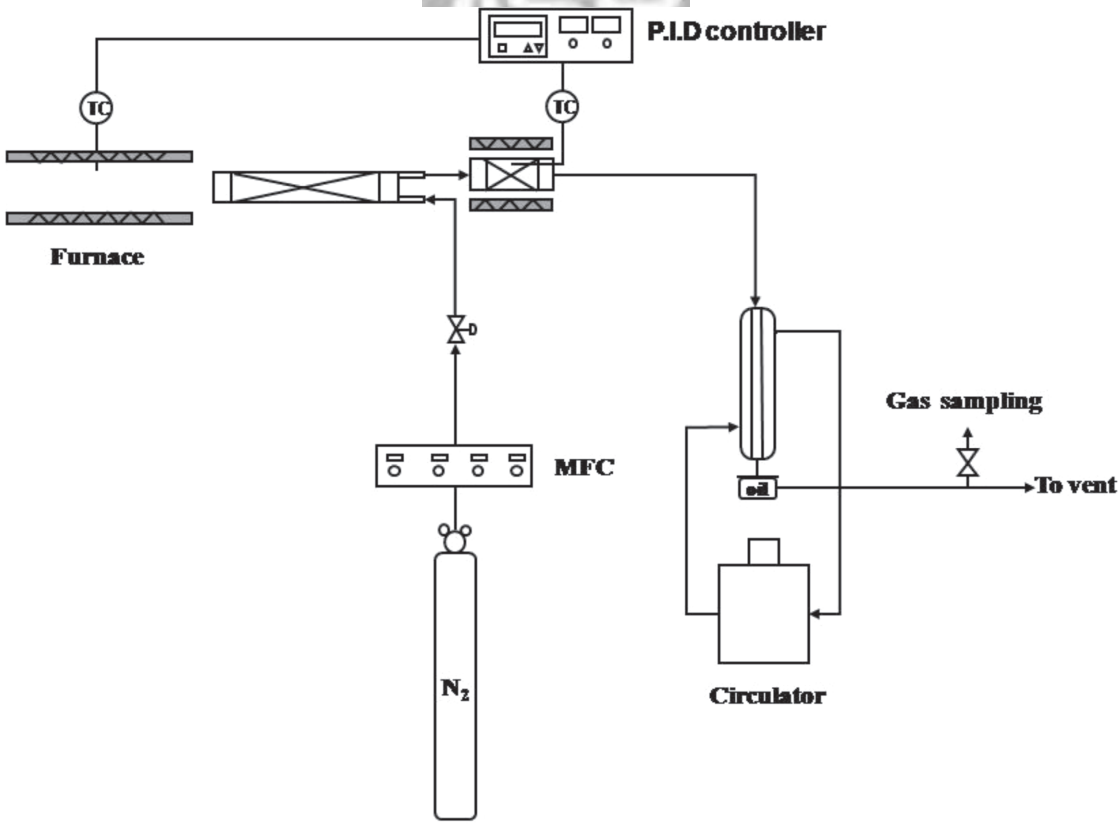

Fig. 1. Schematic diagram of catalytic upgrading apparatus.

apparatus. The fixed catalyst bed system was consecutively installed at the latter part of the main pyrolysis reactor. The main pyrolysis reactor was a U-type quartz with an inner volume of 50 mL, a height of 160 mm, and an internal diameter of 15 mm, into which the Japanese larch sawdust (5.0 g) was charged. The fixed catalyst bed reactor was of the tubular quartz type, with a height of 70 mm and an internal diameter of 15 mm, and it was filled with the catalyst (0.5 g). For use in the experiments, all the catalysts were pelletized, crushed, and screened with standard sieves (1.7–2.4 mm). For the non-catalytic pyrolysis, the catalyst was replaced with quartz beads to maintain the same space velocity within the fixed catalyst bed. Prior to the experiments, all the experimental systems were purged with inert nitrogen at a flow rate of 50 mL/min for 1 h. All the reactors were indirectly heated electrically to the desired reaction temperature. After the two reaction temperatures reached 500 °C, the main pyrolysis reactor was inserted into the furnace. Thereafter, the upgrading reaction continued for 1 h. The temperatures of the experimental systems were adjusted using a PID temperature controller and monitored with 2 thermocouples (K type). The errors of their average reaction temperatures were within ±5 °C. The apparent residence time of the vapors in the main pyrolysis reactor was ~5 s. Condensable bio-oil was collected in a glass condenser cooled to a temperature of −25 °C, using a circulator (RW-2025G, JEIO TECH) with ethyl alcohol as the cooling solvent. The non-condensable gases through the quenching system were sampled using Teflon gas bags at 30 min intervals to analyze their composition.

The water contents of the produced bio-oils were measured using the ASTM E 203 method. A Karl Fischer titrator (Metrohm 787 KF Titrino) was used, along with HYDRANAL Composite 5 K (Riedel-de Haen) and HYDRANAL Working Medium K (Riedel-de Haen) as the titration reagent and the titration solvent, respectively. The accuracy of the analysis was <1%. To determine the bio-oils' chemical composition, they were centrifuged at 3000 rpm for 5 min, after which their of organic fractions were separated from their aqueous fractions. Since bio-oil generally contains hundreds of compounds, accurate quantitative analysis results are difficult to obtain using the external standard method with the existing gas chromatography equipment. Therefore, the area % of a GC-MS chromatogram can be considered a good approximation as it indicates the amounts of various chemical compounds in the bio-oil.[17] In this study, quantitative and qualitative analyses of the organic fractions were performed with a GC-MS (HP 5973 *inert*) with a HP-5MS (30 m × 0.25 mm × 0.25 μm) capillary column, and helium used as the carrier gas. The interpretation of the mass spectra obtained via the GC-MS was based on an automatic library search (Wiley 7n). The pyrolysis gases were analyzed using GC-TCD and GC-FID (ACME 6000, Young Lin Instrument Co., Ltd.) that employed a Carboxen 1000 column (15 ft × 1/8 in) and an HP-plot Al_2O_3/KCl column.

3. RESULTS AND DISCUSSION

3.1. Characterization of Catalysts

Figure 2 shows the nitrogen adsorption–desorption isotherms of the mesoporous catalysts. The Meso MFI C16 zeolite isotherm shows an increase in the adsorption in the range of $P/P_0 = 0.7 \sim 0.8$, whereas $MMZ_{ZSM\text{-}5}$ exhibited an isotherm similar to that of the typical mesoporous material, MCM-41. This suggests that the Meso MFI C16 zeolite has a higher textural porosity than $MMZ_{ZSM\text{-}5}$. Table I shows the textural properties of the catalysts used. The BET surface area and the pore volume of the Meso MFI C16 zeolite were much higher than those of the conventional HZSM-5 zeolite. This was attributed to the formation of mesopores, as described in a previous study.[16] In addition, the pore size of the Meso MFI C16 zeolite was larger than that of the $MMZ_{ZSM\text{-}5}$ material. This indicates that this porosity can allow large molecules, such as pyrolytic vapors derived from the lignocellulosics to diffuse inside the pores. Figure 3 shows the NH_3-temperature programmed desorption (TPD) curves of the catalysts. The Meso MFI C16 zeolite has a large amount of Brönsted acid sites, the active sites in the cracking reaction of the pyrolytic vapors, similar to that of HZSM-5, unlike the $MMZ_{ZSM\text{-}5}$ material. More detailed characterization data on the structure and morphology of the mesoporous catalysts used in this study are reported elsewhere.[13, 15, 16]

3.2. Catalytic Pyrolysis of Japanese Larch

Table II shows the product distributions after the catalytic pyrolysis of Japanese larch. Both the total bio-oil and the organic fraction yield were significantly lower due to the catalytic cracking of the pyrolytic vapors. On the other

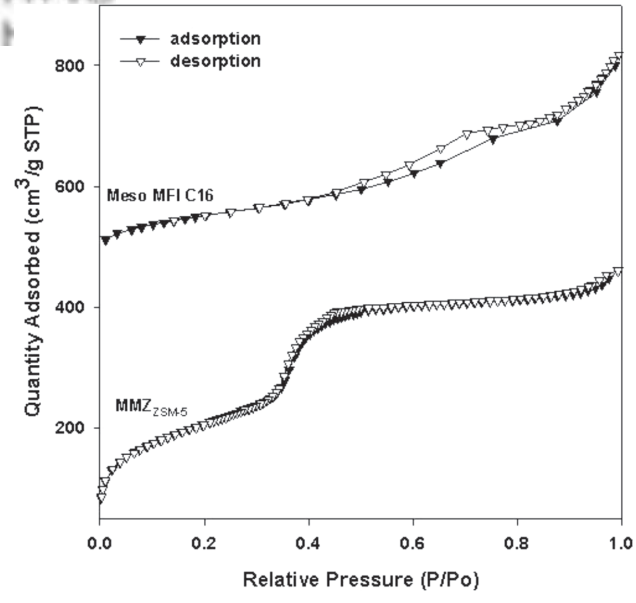

Fig. 2. N_2 adsorption–desorption isotherms of mesoporous catalysts.

Table I. Textural properties of catalysts used in experiments.

Sample	HZSM-5	MMZ_{ZSM-5}	Meso MFI C16
Si/Al[a]	20.1	18.2	18.3
S_{BET}[b] ($m^2\ g^{-1}$)	450	850	527
S_{micro}[c] ($m^2\ g^{-1}$)	295	—	198
V_P[d] ($cm^3\ g^{-1}$)	0.28	0.72	0.62
V_{micro}[e] ($cm^3\ g^{-1}$)	0.14	–	0.09
d[f] (nm)	—	2.7	6.2

[a]Measured by ICP-AES analysis. [b]Calculated in the range of relative pressure $(P/P_0) = 0.05–0.20$. [c]Micropore surface area evaluated by the t-plot method. [d]Measured at $P/P_0 = 0.99$. [e]Micropore volume evaluated by the t-plot method. [f]Mesopore diameter calculated by the BJH method.

Table II. Product distribution from catalytic pyrolysis of Japanese larch.

Catalyst	Non-catalytic	HZSM-5	MMZ_{ZSM-5}	Meso MFI C16
Product distribution (wt%)				
Bio-oil				
Total	56.2	46.8	49.0	42.6
Organic fraction	19.5	13.9	16.0	11.1
Water content[a]	36.9	50.6	49.5	60.3
Gas	21.2	30.4	27.3	34.6
Char	22.6	22.8	23.7	22.8
Coke[b] (wt%)[c]	—	14.2	18.5	21.2

[a]wt% on total bio-oil basis. [b]Obtained by TGA experiments of catalyst after reaction. [c]wt% on catalyst weight basis.

hand, there was an increase in the gas yield, compared with the non-catalytic pyrolysis. With the use of catalysts, the water content in the bio-oils also increased significantly. This was attributed to the deoxygenation of the bio-oil. The proton of the catalyst could react with the oxygen of the bio-oil and produce water by hydrogen transfer.

Of the catalysts examined, the Meso MFI C16 zeolite showed the most pronounced cracking activity due to the synergic effect of its high porosity and its strong acidic properties, particularly in the deoxygenation of the oxygenated compounds in the bio-oil. The degree of deoxygenation of the MMZ_{ZSM-5} material was lower, however, than of the microporous HZSM-5, even though it contained mesopores. This indicates that the acidic properties of the catalytic pyrolysis of Japanese larch are more preferable than the porosity. After the catalytic pyrolysis, the amount of coke deposited on the catalyst depended significantly on the pore size. This was because the large pores of the catalyst were favorable for the formation of larger molecules, which can act as the precursor of coke.

3.3. Chemical Composition of Upgraded Bio-Oils

In this study, the chemical composition of bio-oil was largely divided into undesirables, such as oxygenates and polycyclic aromatic hydrocarbons (PAHs), and desirables such as mono aromatics and phenolics. Figure 4 shows the chemical composition of the bio-oils obtained through non-catalytic pyrolysis and catalytic pyrolysis of Japanese larch.

Using the catalysts, the undesirable oxygenates were reduced significantly, particularly in the case of the zeolites with strong acidic properties. In addition, the strong acidic zeolites produced various aromatic hydrocarbons. In particular, the Meso MFI C16 zeolite exhibited more excellent selectivity for the production of mono aromatics (60% of which were BTX aromatics that are important chemicals in petrochemical industries) than HZSM-5 due to the easier accessibility of the large molecules. However, the Meso MFI C16 zeolite produced more undesirable PAHs than the conventional HZSM-5 due to the presence of mesopores that play an important role in the formation of larger molecules as mentioned earlier. In this study, the polar phenolics are not discussed because only the organic fractions that were separated were analyzed, even though phenolics can be also considered desirable compounds.

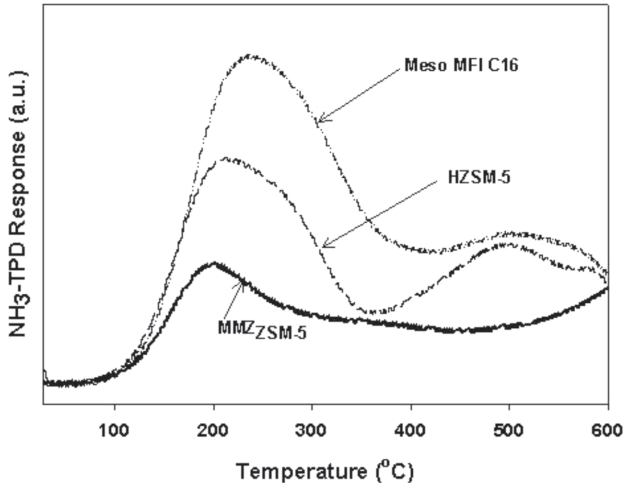

Fig. 3. NH_3-TPD curves of catalysts.

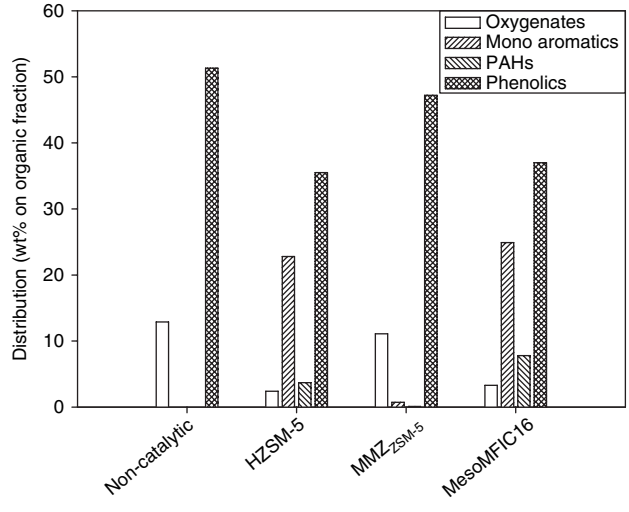

Fig. 4. Chemical composition of bio-oils.

Table III. Composition of gas products.

	Yield (wt%)			Selectivity (%)						
	CO	CO_2	C_1–C_4	CH_4	C_2H_4	C_2H_6	C_3H_6	C_3H_8	C_4H_8s	C_4H_{10}s
Non-catalytic	7.2	11.2	2.8	60.8	8.2	11.1	8.3	5.4	5.3	0.8
HZSM-5	11.0	16.0	3.4	46.5	18.5	9.2	14.0	4.3	6.3	1.2
MMZ_{ZSM-5}	14.3	9.1	3.9	57.6	10.2	11.1	9.8	4.8	5.7	0.8
Meso MFI C16	14.3	15.6	4.7	40.7	15.7	8.8	22.7	3.4	7.5	0.9

3.4. Gaseous Products

The uncondensable gas products were analyzed quantitatively by GC-TCD and GC-FID. The results are shown in Table III. The main products were CO, CO_2 and low molecular hydrocarbons within the range of C_1–C_4. In this study, the amount of hydrogen was negligible (less than 0.2 wt%). The amount of CO and CO_2 increased significantly with the use of catalysts. This indicates that the oxygen in bio-oil can be transformed into CO and CO_2 as well as into H_2O. In addition, the amount of alkanes and alkenes increased after the catalytic pyrolysis but there was a considerable difference in the distribution of each component according to the catalysts examined. In the case of strong acidic zeolites, there was a decrease in the concentration of alkanes, such as methane and ethane, whereas there was a considerable increase in the concentration of alkenes increased, particularly of ethene and propene. This is associated with the amount of aromatics, as previously observed in the chemical composition of bio-oils, and can be described using the following protolytic mechanism.[8] The C_2–C_4 alkenes produced from the protolysis of the light alkanes and the direct decomposition of the pyrolytic vapors undergo successive oligomerization, cyclization, and dehydrogenation. These are finally transformed into aromatic hydrocarbons. From this mechanism, it can be deduced that the concentration of aromatics depends on the concentration of alkenes, which are the precursors of aromatics in the reaction mixture. The results in this study support this deduction.

4. CONCLUSION

Hierarchical MFI zeolite exhibited the most pronounced activity both in deoxygenation and aromatization during the catalytic pyrolysis of Japanese larch. This was attributed to the synergic effect of its high porosity and acidity. In particular, the hierarchical MFI zeolite showed high selectivity for highly valuable chemicals, such as BTX aromatics, even though it decreased the chemicals' organic fraction and total bio-oil yield. Unfortunately, however, the hierarchical MFI zeolite's higher mesoporosity increased both the coke amount and the concentration of undesirable products, such as PAHs.

Acknowledgment: This study was supported from the 2008 grant of The University of Seoul.

References and Notes

1. P. D. Chantal, S. Kaliaguine, J. L. Grandmaison, and A. Mahay, *Appl. Catal.* 18, 133 (**1985**).
2. R. K. Sharma and N. N. Bakhshi, *Bioresour. Technol.* 45, 195 (**1993**).
3. J. D. Adjaye and N. N. Bakhshi, *Fuel Process. Technol.* 45, 161 (**1995**).
4. J. D. Adjaye and N. N. Bakhshi, *Fuel Process. Technol.* 45, 185 (**1995**).
5. P. T. Williams and N. Nugranad, *Energy* 25, 493 (**2000**).
6. S. Vitolo, B. Bresci, M. Seggiani, and M. G. Gallo, *Fuel* 80, 17 (**2001**).
7. A. A. Lappas, M. C. Samolada, D. K. Iatridis, S. S. Voutetakis, and I. A. Vasalos, *Fuel* 81, 2087 (**2002**).
8. H. J. Park, J. I. Dong, J. K. Jeon, K. S. Yoo, J. H. Yim, J. M. Sohn, and Y. K. Park, *J. Ind. Eng. Chem.* 13, 182 (**2007**).
9. K. Ariga, J. P. Hill, M. V. Lee, A. Viny, R. Charvet, and S. Acharya, *Sci. Technol. Adv. Mater.* 9, 014109 (**2008**).
10. J. Adam, E. Antonakou, A. Lappas, M. Stöcker, M. H. Nilsen, A. Bouzga, J. E. Hustad, and G. Øye, *Micropor. Mesopor. Mater.* 96, 93 (**2006**).
11. E. Antonakou, A. Lappas, M. H. Nilsen, A. Bouzga, and M. Stöcker, *Fuel* 85, 2202 (**2006**).
12. K. S. Triantafyllidis, E. F. Iliopoulou, E. V. Antonakou, A. A. Lappas, H. Wang, and T. J. Pinnavaia, *Micropor. Mesopor. Mater.* 99, 132 (**2007**).
13. H. I. Lee, H. J. Park, Y. K. Park, J. Y. Hur, J. K. Jeon, and J. M. Kim, *Catal. Today* 132, 68 (**2008**).
14. H. J. Park, J. K. Jeon, J. M. Kim, H. I. Lee, J. H. Yim, J. H. Park, and Y. K. Park, *J. Nanosci. Nanotechnol.* 8, 5439 (**2008**).
15. M. Choi, H. Cho, R. Srivastava, C. Venkatesan, D. Choi, and R. Ryoo, *Nat. Mater.* 5, 718 (**2006**).
16. V. N. Shetti, J. Kim, R. Srivastava, M. K. Choi, and R. Ryoo, *J. Catal.* 254, 296 (**2008**).
17. M. C. Samolada, A. Papafotica, and I. A. Vasalos, *Energy Fuels* 14, 1161 (**2000**).

Received: 10 November 2008. Accepted: 30 January 2009.